



Received on 25 September 2019; received in revised form, 06 February 2020; accepted, 10 March 2020; published 01 August 2020

ANTI-WRINKLE ACTIVITY AND UPLC-MS/MS METABOLIC PROFILING OF POMEGRANATE AND GRAPE SEEDS EXTRACTS

Sally M. Odah¹, Maha M. Salama^{2,3}, Wafaa M. Aziz², Taha S. El-Alfy² and Shahira M. Ezzat^{* 2,4}

Academy of Scientific Research and Technology¹, Kasr El-Aini Street, 11516, Cairo, Egypt
Department of Pharmacognosy², Faculty of Pharmacy, Cairo University, Kasr El-Aini Street, 11562, Cairo, Egypt.

Department of Pharmacognosy³, Faculty of Pharmacy, The British University in Egypt, El-Sherouk City, Cairo 11837, Egypt.

Department of Pharmacognosy⁴, Faculty of Pharmacy, October University for Modern Sciences and Arts (MSA), Giza 11787, Egypt.

Keywords:

Punica granatum, *Vitis venifera*,
Antiaging, Waste products, MMP-2

Correspondence to Author:

Shahira M. Ezzat

Professor,
Department of Pharmacognosy,
Faculty of Pharmacy, Cairo
University, Kasr El-Aini Street,
11562, Cairo, Egypt.

E-mail: shahira.ezzat@pharma.cu.edu.eg

ABSTRACT: UV irradiation is one of the main causes of what is known as photoaging characterized by loss of skin elasticity and the appearance of wrinkles. In this study, the anti-wrinkle activity of grape seed extract (GSE) and Pomegranate seed extract (PSE) was studied through evaluation of their *in-vitro* antioxidant, anti-tyrosinase and *in-vivo* anti-wrinkle activity in UVB-irradiated mice through topical application of PSE and GSE at 50 mg/kg/twice a week for 15 weeks. The total phenolic content of PSE and GSE was 2.1375 and 5.9625 mg GAE/g extract, respectively. PSE and GSE also showed DPPH scavenging activity with IC₅₀ of 37.9 and 29.9 µg/mL, respectively. PSE and GSE showed anti-tyrosinase activity with IC₅₀ of 115 and 107.75 µg /mL, respectively, while that of Kojic acid is 17.45 µg /mL. In UVB-irradiated mice, the increased expression of metalloproteinase (MMP-2) was significantly inhibited by PSE and GSE where their activities exceeded that of the standard turmeric extract (TME). The topical application of PSE, GSE, and TME of the UVB radiated groups prevented the increase in the thickness of the epidermis induced by UVB. UPLC-MS/MS profiling of both extracts led to the identification of 43 phenolic compounds of different classes. We can conclude that the anti-wrinkle activity of both extracts was attributed to their high phenolic content and the antioxidant potential of both extracts. Therefore, the seeds of pomegranate and grapes, which are considered as waste products, could be incorporated in cosmeceutical skincare products after further clinical trials.

INTRODUCTION: Plastic surgery is nowadays drawing attention to patients suffering from aging problems. Aging of the skin is basically due to two main factors, either genetic or environmental.

Long term exposure of ultraviolet radiation, excessive smoking, windy weather, and chemicals application cause signs of aging as sagging, roughness, fine lines, irregular pigmentation, and loss of skin elasticity¹. Chronic exposure to the sun results in UV-induced skin damage; this phenomenon is known as photoaging. The signs of photoaging are mainly illustrated by histological changes; these are expressed as damage to collagen fibers and extreme elastic fibers deposition². All these lead to a wrinkled, coarse, rigid skin, with uneven pigmentation and brown spots³.

<p>QUICK RESPONSE CODE</p> 	<p>DOI: 10.13040/IJPSR.0975-8232.11(8).3679-89</p> <hr/> <p>This article can be accessed online on www.ijpsr.com</p> <hr/> <p>DOI link: http://dx.doi.org/10.13040/IJPSR.0975-8232.11(8).3679-89</p>
---	---

Ultraviolet light is primarily absorbed in the epidermis, which is mainly formed of keratinocytes. UV-induced aging factors are released in the epidermis⁴. These factors impair the synthesis of collagen inducing matrix metalloproteinases (MMPs)⁵. MMPs are zinc-dependent endopeptidases; they are capable of degrading all extracellular matrix proteins (ECMs)⁶. Matrix metalloproteinases are classified into five families: the most important of which are collagenases family in addition to gelatinases, stromelysins, matrilysins, and membrane-type MMP families. Alteration of the skin is mediated through these enzymes that cause the degradation of collagens, proteoglycans, and different glycoproteins⁷. Remodeling of the extracellular matrix is usually intervened through MMPs. Hence, MMPs could contribute to skin ulcers, arthritis, morphogenesis, angiogenesis, photoaging, and finally, skin cancer⁸.

Skin, including fibroblasts, are greatly affected by ultraviolet radiation, as these radiations, even in relatively low concentration, can enhance the expression of MMP-1, -2, -3, and -9 enzymes in the skin⁹ leading to the degradation of collagen. Therefore, MMPs are known as UVB-induced aging factors⁸. MMP-2 and MMP-9 are highly expressed in wrinkle bearing skin, whereas MMP-1 and MMP-3 are present in non-irradiated skin than irradiated skin. Consequently, chronic exposure to UVB upregulate MMP-2 and MMP-9 release in the skin, causing wrinkles and skin damage⁹.

Cosmetics prepared from herbs are nowadays drawing attention in different areas due to their safety and their reputed effect on the skin, especially skin aging. Skin formula rich in natural products have high absorptivity and low allergic reaction on the skin. These herbal drugs are usually rich in polyphenols with high antioxidant potential, hence can scavenge free radicals which contribute collagen damage. Furthermore, the intake of these herbs as a diet is a useful tool for a healthy body as well as delaying the signs of aging through their antioxidant effect. It was reported that the bioactive fractions rich in phenolic compounds of pomegranate could be used as a skin repair agent. In addition, a water-soluble fraction made from pomegranate peel was found to inhibit MMP-1¹⁰. Another report dealt with the ant-aging activity of

the rosemary extract; results revealed that the high anti-wrinkle activity of the phenolic rich extract, this activity was further enhanced on incorporating the extract in a nanoparticle¹¹. Herein, we have studied the effect of PSE (pomegranate seed extract) and GSE (grape seed extract) compared to TME (turmeric methanolic extract) as a reference extract, on chronic UVB irradiated- induced skin damage including changes in skin thickness and wrinkling in hairless mice, applying matrix metalloproteinase gene expression method.

Moreover, antioxidant activity was tested for both extracts. A comprehensive chemical profile of the defatted methanolic extracts for both pomegranate and grape seeds using UPLC-ESI-MS/MS was also performed.

MATERIALS AND METHODS:

Plant Material: Plant material of the seeds of both pomegranate (*Punica granatum* L. F. Lythraceae) and grape (*Vitis venifera* L. Vitaceae) was collected all over the years (2014-2016) from Horticulture Research Institute. Pomegranate seeds were kindly identified by Dr. Mohammed El-Sayed as wonderful variety, and grapes were identified by Dr. Aisha Salah as red romy variety. Voucher specimens for both pomegranate and grapes (24.1.2016 and 25.1.2016), respectively, were kept in the herbarium of the Department of Pharmacognosy, Faculty of Pharmacy Cairo University.

Extraction Procedure: The air-dried powders of both pomegranate and grape seeds (0.5 Kg) were exhaustively defatted using *n*-hexane in a soxhlet apparatus (each separately). Each of the dried defatted seeds was separately extracted with acetone: water: acetic acid (90: 9.5: 0.5) using soxhlet apparatus 60 - 70 °C. The solvent in each case was evaporated under reduced pressure at a temperature not exceeding 60 °C till complete dryness to yield 52 and 60 g of pomegranate seed extract (PSE) and grape seed extract (GSE), respectively.

Quantitative Estimation of Total Phenolic Content: Spectrophotometric determination of the total phenolic content for GSE and PSE was carried out using the Folin-Ciocalteu colorimetric method¹². Total phenols were expressed as mg of Gallic Acid Equivalents (mg GAE)/g of the dry extract.

In-vitro Antioxidant Activity:

2, 2- Diphenyl-1-Picrylhydrazyl (DPPH) Free Radical Scavenging Assay: The free radical scavenging activities of PSE and GSE were assessed against 2, 2, Diphenyl-1-Picrylhydrazyl (DPPH)¹³.

Anti-tyrosinase Assay: Tyrosinase inhibitory activity is determined spectrophotometrically¹⁴. Tyrosinase inhibitory activity of GSE and PSE was determined and compared with the activity of standard Kojic acid.

In-vivo Anti-Wrinkle Activity:

Animals: Thirty male Swiss albino mice weighing 25 ± 5 g were obtained from the animal house of the National Research Center. The hair of the dorsal sides of the mice was shaved, and all experiments were performed during the light phase of the light/dark cycle after a week of acclimatization. The procedures adopted for the experiments were done in compliance with the regulations stated by the laboratory animal handling and in agreement with the Ethics Committee's Ethics, Faculty of Pharmacy, Cairo University, Cairo, Egypt (PI 1894).

Experimental Design: To evaluate the effect of PSE, GSE and TME on skin wrinkles, the thirty mice were allocated into five groups, group I served as normal control, the back of shaved mice in group II-V was subjected to a UVB lamp (15 W type, UV maximum wavelength 254 nm, UV intensity 100 mW/cm^2 , Ieda Boeki Co., Tokyo, Japan) for 5 min. daily/15 weeks. Wrinkles were to be observed macroscopically in the dorsal region from at week 15 after the initiation of UV irradiation. After this period, group II served as a UVB irradiated untreated group; groups III, IV, and V were treated with PSE, GSE, and turmeric methanolic extract (TME) which serves as a reference extract, respectively. The extracts were applied topically at 50 mg/kg/twice daily for 15 weeks. Regarding the evaluation of wrinkles, the intraperitoneal injection was achieved to induce anesthesia per each mouse. The degree of wrinkles on the dorsal area was measured according to the wrinkle score **Table 1**. This method is modified by Bisset *et al.*, 1987, to assess the grading scale; the high grading scale ($\Rightarrow >3$) indicates development of deep wrinkles.

Histological Examination: Dorsal skin samples were fixed in 10% buffered formalin for at least 24 h, progressively dehydrated in solutions containing an increasing percentage of ethanol (70, 80, 95 and 100%, v/v) cleared in histoclear, embedded in paraffin under vacuum, sectioned $5 \mu\text{m}$ thick deparaffinized, and stained with hematoxylin-eosin.

Measurement of MMP-2 and MMP-9 Gene Expression in UVB Irradiated Mice: This was achieved by Real time-Polymerase Chain Reaction (Real Time-PCR)^{15,16}.

UPLC-ESI-MS/MS Analysis of the GSE & PSE Extracts:

GSE: Chromatographic technique was performed by means of an Agilent 6420 triple quad UPLC system (Agilent, California, USA) equipped with Acquity BEH shield Rp 18 column (1500×2.1 mm, particle size $1.7 \mu\text{m}$, Waters Milford, USA). The mobile phase applied for isolation: 0.2% formic acid in water and (A) and acetonitrile (B). The elution was done as follows: 0.95 mL min⁻¹ gradient solvent B: 0-20 min, 5-16%; 20-28 min, 16-40%; 28-32 min, 40-70%; 32-36 min, 70-99%; 36-45 min, 99% and 45-46, min. 99-5%.³⁰ The injection volume was 10 μL .

PSE: A dual mobile phase compiling 2% (v/v) acetic acid in water (A) and 0.5% acetic acid in water and methanol (10/90, v/v; B). The flow rate was adjusted at 0.4 mL/min, while the gradient program was enhanced to: 0-2% B (13 min), 2-5% B (5 min), 5-10% B (5 min), 10-25% B (20 min), 25-50% B (10 min), 50-100% B (5 min), 100% B isocratic (5 min), 100-0% B (3 min), 0% B isocratic (5 min). Run time was 71 min totally. Different wavelengths were set to measure different classes; 280 nm (for flavan-3-ols and benzoic acid derivatives), 360 nm (for flavonols and cinnamic acid derivatives), and 520-600 nm (for anthocyanin and anthocyanin derivatives). The eluted compounds were scanned from m/z 50 to 1000, with the aid of an MS QQQ mass spectrometer equipped with an electrospray ion source in the negative ion mode. The instrument settings used were; nebulizer gas, nitrogen, 40 psi; dry gas, nitrogen, 10 mL/min, 300 °C; capillary, -3000 V (+4000 V); endplate offset, -500 V; funnel 1 RF, 200 Vpp; funnel 2 RF, 200 Vpp.

Identification of the metabolites of the studied plants was achieved by detecting their retention times, their mass spectra, and comparison with reference literature as well.

RESULTS AND DISCUSSION: Tyrosinase enzyme is considered a crucial step in the biosynthesis of melanin. Tyrosine could be transferred into L-dopa, then transformed to dopaquinone, and finally *via* numerous polymerization reactions-eumelanin and pheomelanin are formed¹⁴. Bioactive extracts, as well as their active metabolites, were found to block this pathway and reduce the formation of melanin, these compounds can be used in skin brightening¹⁶. In our findings, PSE and GSE had a moderate inhibitory effect on the tyrosinase enzyme. The IC₅₀ for PSE and GSE were 115 and 107.75 µg /mL, respectively, while that of Kojic acid is 17.45 µg /mL. Our results also showed that both extracts are rich in phenolics as they showed TPC of PSE and GSE of 2.1375 mg GAE/g and 5.9625 mg GAE/g extract, respectively. Accordingly, the extracts showed strong free radical scavenging activity against DPPH with IC₅₀ values of 37.9 and 29.9 µg/mL of PSE and GSE, respectively, while that of ascorbic acid was 7.55 µg/mL.

Photoaging is characterized by notable signs such as the increase in the thickness of the skin, and the firmness of the skin is reduced. Moreover, histological alterations occur, revealing collagen damage accompanied by massive abnormal elastic fibers settlement. This is further associated with an increase in the expression of MMP-2. The histological examination showed that the topical application of PSE and GSE (at 50 mg/kg/twice a day for 15 weeks) prevented an increase in the thickness of the epidermis, and no effect was observed on extracellular matrix (ECM) of the corium induced by chronic UVB exposure. The results also showed a significant difference between treated and untreated groups as PSE and GSE had an inhibition effect on the increase of the expression of MMP-2 as regards to the UVB radiated group.

The expression of MMP-2 was increased by UVB irradiation compared to levels of the UVB irradiated group. The increased expression of MMP-2 was significantly inhibited by PSE, GSE,

and TME, as described in **Table 1**. It is worthy to note that the effect of PSE and GSE exceeded that of the standard TME.

TABLE 1: RESULTS FOR WRINKLE SCORES, MMP-2 AND MMP-9 FOR THE CONTROL GROUP, UVB RADIATED GROUP, PSE EFFECT ON THE UVB RADIATED GROUP, GSE EFFECT ON THE UVB RADIATED GROUP AND TME EFFECT ON THE UVB RADIATED GROUP

Extract	Wrinkle score	MMP-2	MMP-9
UVB	3.7±0.23*	0.72±0.08*	1.28±0.2*
Normal control	0±0*	0.12±0.02*	0.54±0.03*
PSE	2.08±0.22*	0.37±0.05*	0.52±0.09*
GSE	2.7±0.17*	0.23±0.01*	0.52±0.09*
TME	2.73±0.23*	0.47±0.79*	0.66±0.12*

Mean for UVB radiated, control, PSE, GSE, and TME; *standard error (SE) for 4 mice. UVB: irradiated group; PSE: pomegranate seed extract; GSE: grape seed extract TME: turmeric methanolic extract. Wrinkle scores: shallow, coarse wrinkle across the back (Bisset's Grade 1); Grade 4 shallow, coarse wrinkle across the entire back (Bisset's Grade 2); Grade 6 some deep, long wrinkles across the back (Bisset's Grade 3).

The histological observation, the thickness of the epidermis, and the extracellular matrix (ECM) of the corium were significantly increased by UVB irradiation. The topical application of PSE, GSE, and TME of the UVB radiated groups (at 50mg/kg/twice a week for 15 weeks) prevented an increase in the thickness of the epidermis and no effect was observed on extracellular matrix (ECM) of the corium induced by chronic UVB exposure **Fig. 1**. All these results support the anti-aging activity of the tested extracts.

UPLC/MS was applied for secondary metabolites profiling of PSE and GSE. Results evidenced that applying the atmospheric pressure *via* negative mode increases the sensitivity of the studied compounds rather than the positive mode. Peaks' selection was based on the major peaks as well as the literature review. The phenolic compounds in PSE and GSE were classified by comparing their UV-vis spectra with that of the reported phenolics as well as reports from the literature. The major classes identified in both extracts under investigation were hydroxycinnamic acid conjugates, flavonoids, benzoic acid conjugates, delphinidin and cyanidin derivatives. Each compound identified per class was achieved on the basis of the chromatographic compartment, its UV-vis as well as its mass spectrum, in addition to, comparison to the published literature. **Table 2**, **Fig. 2** and **3** display a summary and discussion for the results. A total of 47 metabolites were detected, of which 43 were identified.

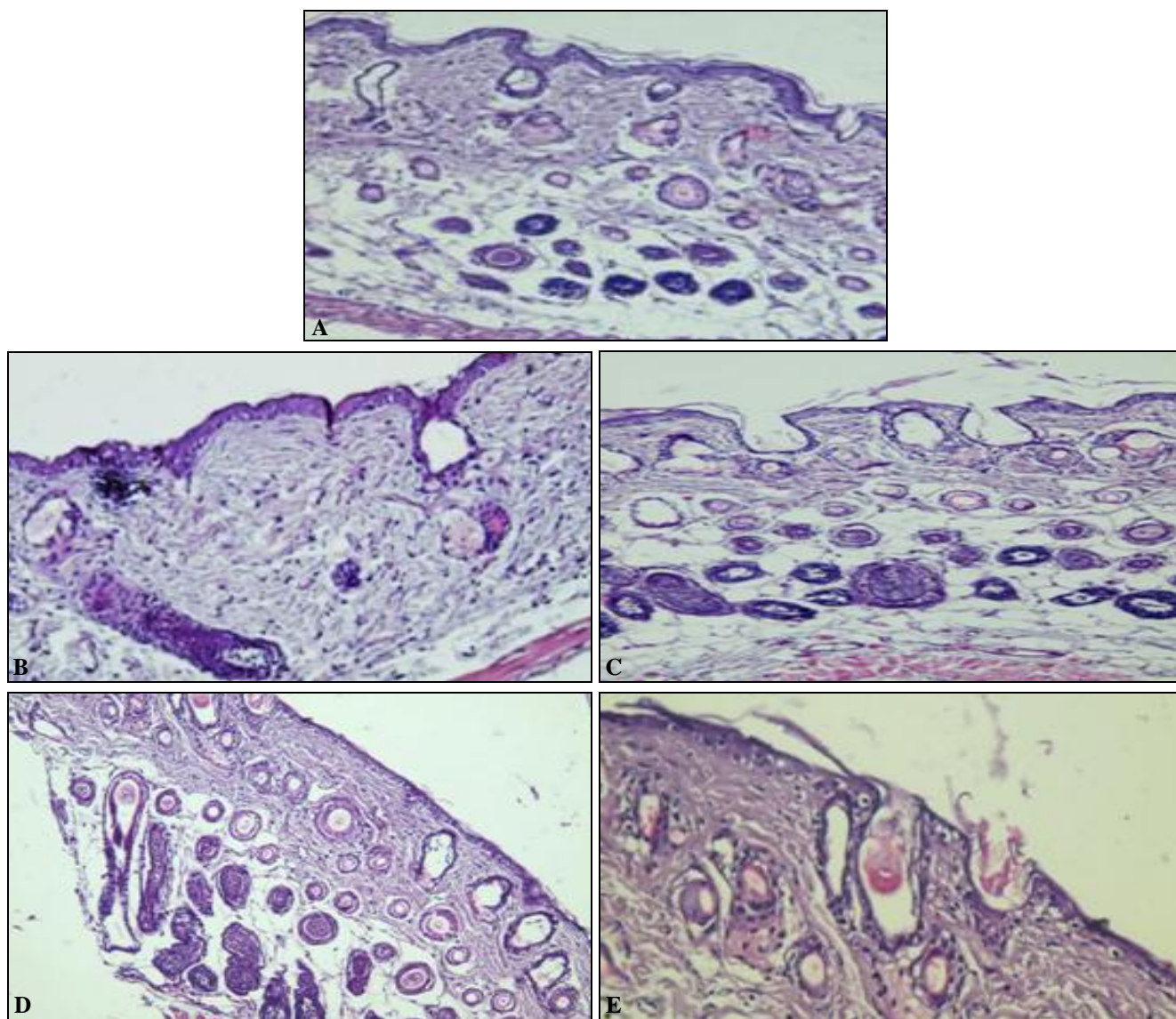


FIG. 1: HISTOPATHOLOGICAL EXAMINATION OF MICE SKIN. A NORMAL SKIN THICKNESS; B, IRRADIATED SKIN THICKNESS WITH INCREASED THICKNESS (UNTREATED); C, EFFECT OF PSE OF IRRADIATED SKIN ON SKIN THICKNESS; D, EFFECT OF GSE OF IRRADIATED SKIN ON SKIN THICKNESS; E, EFFECT OF TME OF IRRADIATED SKIN ON SKIN THICKNESS

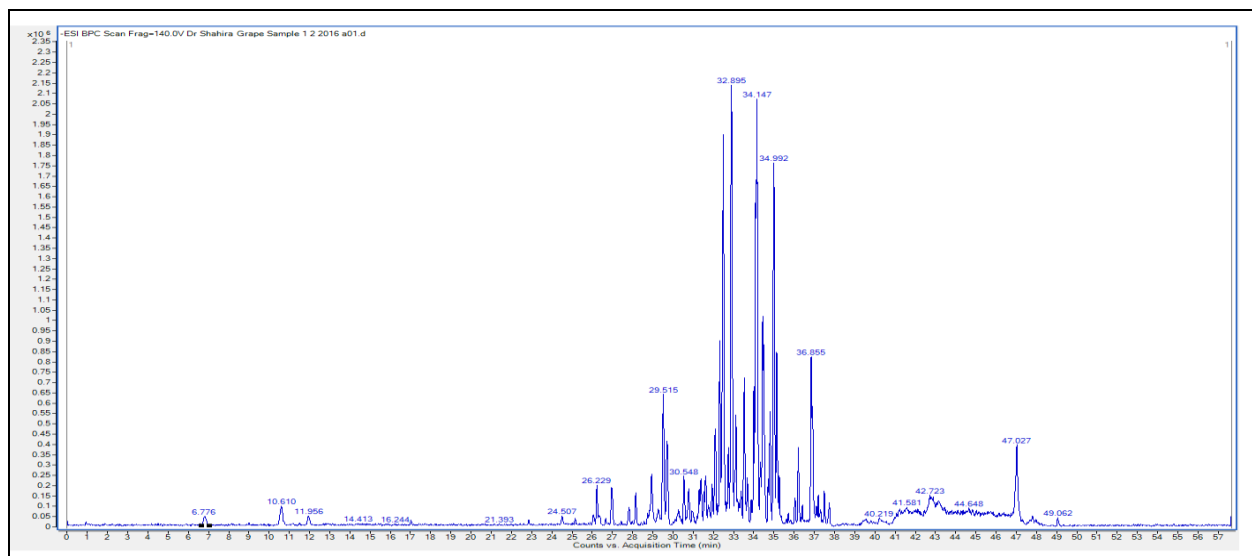


FIG. 2: UPLC CHROMATOGRAM OF GSE

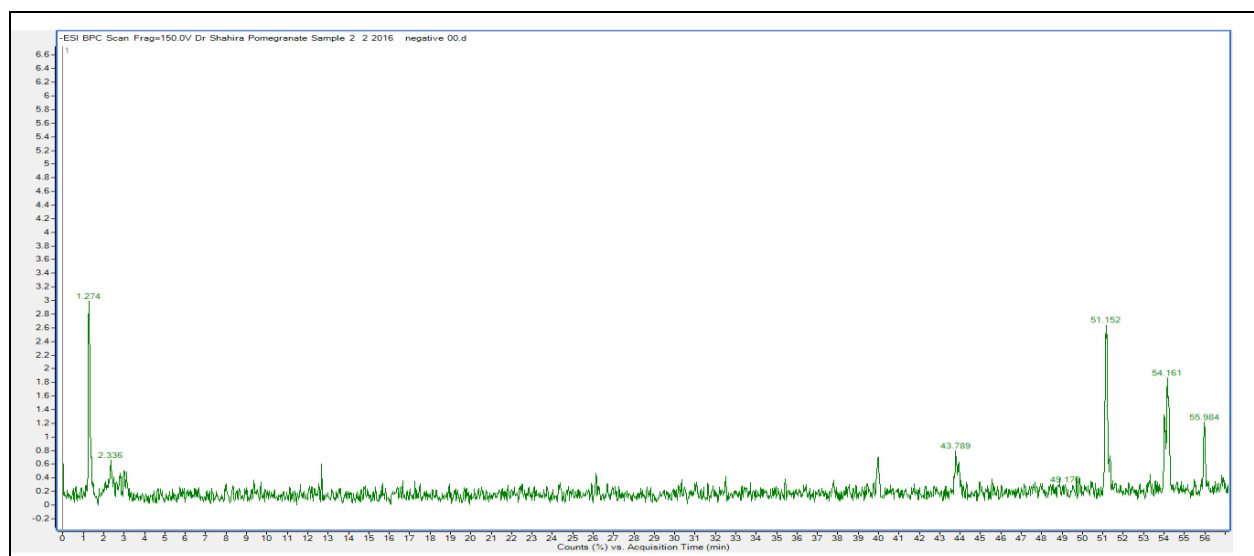


FIG. 3: UPLC CHROMATOGRAM OF PSE

TABLE 2: PEAK ASSIGNMENTS OF METABOLITES IN PSE AND GSE USING UPLC-MS/MS IN NEGATIVE MODE

Peak	t _R (min)	[M-H] ⁻	Molecular formula	Tentative Identification	MS ²	GSE	PSE
1	2.13	109	C ₆ H ₆ O ₂	Catechol	93,65	+	-
2	3.1	169	C ₂₆ H ₃₆ O ₄	Gallic acid	123, 79	+	+
3	3.94	168	C ₈ H ₈ O ₄	Vanillic acid	152, 123	+	-
4	4.1	249	C ₈ H ₁₀ O ₉	Oxydisuccinic acid	205, 133, 113	+	-
5	4.54	315	C ₁₃ H ₁₆ O ₉	Protocatechuic acid hexoside	153, 109	+	+
6	4.87	315	C ₁₃ H ₁₆ O ₉	Gentic acid hexoside	153, 136	+	-
7	5.12	317		Unknown		+	-
8	5.8	289	C ₇ H ₆ O ₅	(epi)Catechin	245, 205, 179	+	+
9	6.3	301	C ₁₄ H ₆ O ₈	Ellagic acid	257, 229, 185	+	+
10	6.77	193	C ₁₀ H ₁₀ O ₄	Ferulic acid	179, 133	+	-
11	9.6	311	C ₁₃ H ₁₁ O ₉	Caftaric acid	179, 149, 135	+	-
12	10.61	325	C ₁₄ H ₁₃ O ₉	Fertaric acid	193, 149	-	+
13	11.95	337	C ₁₆ H ₁₈ O ₈	<i>p</i> -Coumaroylquinic acid	191, 163	-	+
14	14.41	353	C ₁₆ H ₁₈ O ₉	Caffeoylquinic acid	191, 179	-	+
15	16.24	367	C ₁₇ H ₂₀ O ₉	Feruloylquinic acid	349, 193, 191	+	+
16	21.39	341	C ₁₅ H ₁₈ O ₉	Caffeic acid-hexoside(caffeoyl hexoside)	179, 135	-	+
17	24.50	409		Unknown		-	+
18	26.22	385	C ₁₇ H ₂₂ O ₁₀	Sinapic acid hexoside (sinapoyl hexoside)	223, 179	+	+
19	26.96	423	C ₁₉ H ₁₉ O ₁₁	Unknown	405, 255	-	+
20	27.82	1083	C ₄₈ H ₂₈ O ₃₀	Punicalagin (ellagitannin)	781, 601, 301	-	+
21	28.16	712		Unknown		+	-
22	28.93	865	C ₄₅ H ₃₈ O ₁₈	Proanthocyanidin trimer	713, 695, 577, 451, 407	+	+
23	29.28	729	C ₃₇ H ₃₀ O ₁₆	Proanthocyanidin dimer monogallate	603, 577, 441	+	-
24	29.51	434.03	C ₁₉ H ₁₄ O ₁₂	Ellagic acid pentoside	301, 285	+	+
25	29.90	465	C ₂₁ H ₂₁ O ₁₂ ⁺	Delphinidin -hexoside	303	-	+
26	30.28	433	C ₂₁ H ₂₁ O ₁₀ ⁺	Pelargonidin hexoside	271	+	+
27	30.54	419	C ₂₀ H ₁₉ O ₁₀	Cyanidin -pentoside	287	-	+
28	30.7	506	C ₂₃ H ₂₃ O ₁₃	Acetylated derivative of delphinidin hexoside (delphindin hexosyl acetate)	344, 303	-	+
29	31.61	792		Unknown		+	-
30	32.09	468	C ₂₁ H ₁₀ O ₁₃	Valoneic acid dilactone	425, 407, 301	+	-
31	32.48	463	C ₂₁ H ₁₉ O ₁₁	Quercetin hexoside	301, 281	+	+
32	32.69	447	C ₂₁ H ₂₀ O ₁₁	Orientin (Luteolin-8C-	417, 357, 327	-	+

33	33.40	447	C ₂₁ H ₂₀ O ₁₁	glucoside) Kaempferol -hexoside (astragalin)	285	-	+
34	33.52	447	C ₂₁ H ₂₀ O ₁₁	Quercetin- rhamnoside	301(-146, rhamnose), 151	-	+
35	34.14	449	C ₂₁ H ₂₂ O ₁₁	Astilbin (Taxifolin rhamnoside)	303, 287, 153	-	+
36	34.44	433	C ₂₀ H ₁₇ O ₁₁	Quercetin-pentoside	301, 179	-	+
37	34.81	424	C ₁₉ H ₂₀ O ₁₁	Maclurin-3-C-hexoside	405, 255	+	-
38	35.00	463	C ₂₁ H ₂₀ O ₁₂	Myricetin -rhamnoside	317, 179	+	-
39	36.23	431	C ₂₁ H ₂₀ O ₁₀	Genistein hexoside (genistin)	179	+	+
40	36.85	315	C ₁₆ H ₁₂ O ₇	(<i>iso</i>) Rhamnetin	300, 193, 121	+	+
41	37.49	317	C ₁₆ H ₁₃ O ₇ ⁺	Petunidin	287, 279	+	+
42	37.73	321	C ₂₀ H ₁₈ O ₄	Glabrene	303, 295, 279	-	+
43	42.72	268	C ₁₆ H ₁₂ O ₄	Formononetin	253, 238	+	+
44	47.02	253	C ₁₅ H ₁₀ O ₄	Diadzein	209, 199	-	+
45	51.15	221	C ₁₅ H ₁₀ O ₂	Flavone	100	+	+
46	54.16	301	C ₁₅ H ₁₀ O ₇	Quercetin	273, 257, 151, 135	-	+
47	55.98	299	C ₁₆ H ₁₂ O ₆	Diosmetin	284, 255	-	+

Hydroxy Benzoic Acid Conjugates: These compounds displayed UV absorption at λ_{\max} 320 nm. These were represented by four peaks: Peak 3 shows m/z at 168 [M-H]⁻, the main fragments produced were at m/z 152[M-H-15-H]⁻, due to the loss of CH₃ from the methoxy group, and at m/z 123 [M-H-15-H-28]⁻ that is equivalent to decarboxylation. This was tentatively identified as vanillic acid¹⁷. Another two peaks 5 and 6 peak were distinguished, both have [M-H]⁻ at 315 and yielded on fragmentation m/z 153[M-H-162]⁻, and another fragment peak at m/z 136 [M-162-OH amu]. Peak 5 gave a major fragment at m/z 109 (100%), while peak 6 yielded the major fragment at 136 (80%); these fragmentation patterns are characteristic for protocatechuic acid and gentisic acid, respectively. Hence, the two compounds (peaks 5 and 6) were tentatively identified as protocatechuic acid-hexoside and gentisic acid hexoside¹⁸, respectively. Vanillic acid and gentisic acid were reported in GSE, only, while protocatechuic acid was reported in both PSE and GSE. The fourth peak, peak 2 had [M - H]⁻ at m/z 169 with MS² fragmentation ions at m/z 123 indicating the loss of (CHO₂), and m/z 79 correspondings to the loss of (CHO₂⁻ CO₂), this is the typical fragmentation pattern of gallic acid^{19,20}. This compound was spotted in both PSE and GSE.

Hydroxy Cinammic Conjugates: These are hydroxyl cinnamic acid derivatives either conjugated with quinic acid moiety or with tartaric acid moiety. These were classified as:

A- Hydroxy Cinammoyl Tartarates: Peaks 11 & 12 are obvious from the fragments of a tartaric acid (m/z 149) in their MS spectrum. Peak 11 exhibited a molecular ion of m/z 311 conforming to the molecular formula C₁₃H₁₁O₉ and yielding fragments of caffeic acid (m/z 179 amu), tartaric acid (m/z 149 amu) and small fragment resulted from caffeic acid decarboxylation at m/z 135 and was identified as caftaric acid. Similarly, peak 12 presented the same fragmentation pattern as peak 11 except for an extra 14 amu unit, with molecular ion peak 325 [M-H]⁻ at m/z , C₁₄H₁₃O₉ with daughter ions MS² at m/z 193 indicating ferulic acid and 149 for tartaric acid. This compound was characterized as feruloyl tartaric acid (fertaric acid)²¹. Caftaric was detected in GSE, while fertaric was present in PSE

B-Hydroxy Cinammoyl Quinates: Peak 13, 14 and 15 were identified as coumaroylquinic acid, caffeoylquinic acid, and feruloylquinic acid, respectively, peak 13 with parent ion peak m/z 337 [M-H]⁻, and MS² m/z 191 and m/z 163 [*p*-coumaric acid-H]⁻ as the base peak, this is in accordance with fragmentation pattern of coumaroylquinic acid²². Peak 14, m/z 353 [M-H]⁻, corresponding to C₁₆H₁₈O₉, yielded deprotonated quinic acid (m/z at 191 amu) in addition to another major ion corresponding to the hydroxycinnamic acid residue at m/z 179 [caffeic acid-H]⁻. This is tentatively identified as caffeoylquinic acid²². Peak 15 showed a molecular ion [M - H]⁻ at m/z 367, which yielded fragments m/z 349 [M-H-H₂O]⁻, m/z 191 equivalent

to the loss of a feruloyl moiety and the presence of a quinic acid moiety; and m/z 193 [M-H-quinic acid] indicating the presence of ferulic acid moiety. This compound was identified as feruloylquinic acid²¹. Coumaroylquinic acid and caffeoylquinic acid were detected in grapes only; however, feruloylquinic acid was present in both.

C-Hydroxy Cinammoyl Glycosides: This was manifested by two peaks 16 and 18. Peak 16 showed a molecular ion at m/z 341 that produced MS² characteristic major fragment at m/z 179, which is indicative for caffeic acid and the loss of hexose moiety [M-H-162]⁻, in addition to m/z 135 for the decarboxylated caffeic acid after the loss of hexose and (CO)². Hence, this was tentatively identified as caffeic acid hexoside²³ detected in GSE only. Likely, peak 18 with parent ion peak m/z 385 with MS² at m/z 223 amu [M-H-162]⁻ and another at 179 amu [M-H-162-CO]⁻ in conformity with the loss of a hexose molecule and carboxyl group respectively; this compound was regarded as sinapic acid hexoside²³; the compound was present in both PSE and GSE.

Anthocyanins: The compounds concomitant with peaks 25, 26, 27, 28, and 41 showed UV absorption at λ_{\max} 330-500 nm, which suggests that they might be anthocyanin derivatives²⁴. Peak 41 showed a molecular ion at m/z 317 that produced an MS² fragmentation pattern distinguished at 287, corresponding to cyanidin [M-H-30]⁻, which corresponded to a loss of a methoxyl group. Thus, this compound was characterized as petunidin²⁵. Peak 27 with m/z 419 was characterized as cyanidin-pentoside, as it showed a base peak at m/z 287 [M-132]⁻, which corresponds to the loss of a pentose molecule and m/z 287 is equivalent to the cyanidin aglycone²⁶.

Peak 28 was identified as an acetylated derivative of delphinidin hexoside, with a base peak m/z 506 corresponding to [M-H]⁻ it showed two consecutive peaks at m/z 344 (M-162) and 303 [(M-162)-42], indicating the successive loss of hexose then an acetyl group. Peak 25, with a base peak [M-H]⁻ at m/z 465 and was identified as delphinidin-hexoside, where MS² showed peaks at m/z 303 [(M-H)-162] and [(M-H-122)-28] were assigned for the fragmentation pattern of delphinidin²⁵. Another anthocyanin was detected as peak 26; this

compound exhibited a molecular ion at m/z 433 with MS² fragmentation pattern; at m/z 271, corresponding to pelargonidin due to the loss of [M-162], which compared to the loss of hexose. Thus, this compound was characterized as pelargonidin-hexoside²⁷.

Tannins:

A-Condensed Tannins: Peak 8 with [M-H]⁻ at m/z 289 had daughter MS² ions at m/z 245 due to the loss of COO, other fragments at m/z 205, and 179 due to the cleavage of the ring-A of flavan-3-ol²⁸. This compound was identified as (*epi*)catechin. Peak 22 had [M-H]⁻ at m/z 865 characteristic to procyanidin trimers, it showed daughter MS² ions at m/z 713 due to the loss of 152 amu during the retro-Diels-Alder (RDA) fragmentation of the heterocyclic ring and a base ion peak at m/z 695 corresponding to loss of 170 amu, due to the retro-Diels-Alder (RDA) fragmentation with the loss of H₂O. The internal bond cleavage of the flavan ring appeared by the fragment ions at m/z 577 due to the loss of 288 amu.

The fragmentation pattern of the procyanidin dimers appeared as two fragments at m/z 451 and 407. Peak 23 with molecular ion peak [M-H]⁻ at m/z 729 with MS² daughter ions at m/z 577 due to the loss of a galloyl moiety [M-H-152]⁻, m/z 441 [M-H-288]⁻ due to the loss of an *epi*-catechin, and m/z 603 [M-H-126]⁻ due to the elimination of ring – A. This compound was identified as procyanidin dimer gallate²⁸.

Peak 20 with a molecular ion peak [M-H]⁻ at m/z 1083, characteristic for punicalagins, the main ellagitannins identified in pomegranate juices. It showed the fragmentation pattern characteristic to punicalagin with daughter ions MS² at m/z 781 (gallagyl-hexose) corresponding to the loss of ellagic acid, and m/z 601 (gallagyl)²⁹. Peak 24 displayed [M - H]⁻ at m/z 433 and yielded daughter ions in the negative mode at m/z 301 (M- 132), characteristic to the loss of a pentose moiety, in addition to the typical fragments of ellagic acid at m/z 229 and 185. Similarly, peak 9 had a molecular ion peak [M - H]⁻ at m/z 301 and daughter MS² ions at m/z 257, 229, and 185, consistent with ellagic acid. Finally, peak 30 with a molecular ion peak [M-H]⁻ at m/z 468, with product ions at m/z 425 and 407, consistent with the subsequent loss of a

carboxyl group then H₂O. Furthermore, an ion fragment at (*m/z* 301) matching with the typical fragmentation pattern of ellagic acid. This compound was identified as valoneic acid dilactone³⁰.

O/C-Flavonoid: Three peaks were identified as kaempferol, quercetin derivatives due to their UV spectra and MS fragmentation ions in the negative mode. Peak 33, showed a molecular ion of *m/z* 447, which yielded a daughter fragment of *m/z* 285, assigned to kaempferol aglycone with a loss of 162 amu (a hexose moiety), and was tentatively identified as kaempferol-hexoside (astragalin)³¹.

Peaks 31, 34, 36 & 45 assigned for quercetin derivatives; peak 31 molecular ion of *m/z* 463, yielding a fragment ion of *m/z* 301, assigned to quercetin aglycone with a loss of 162 amu (a hexose moiety), and was tentatively identified as quercetin-hexoside (isoquercitrin)³¹. Peaks 34 and 36 with molecular ion at *m/z* 447 and *m/z* 433, respectively. Both gave a major fragment ion at *m/z* 301, indicating the loss of either [M-H-146 (rhamnose)] from peak 34 or [M-H-132 (pentose)] from peak 36. Accordingly, peaks 32 and 36 were characterized as quercetin rhamnoside and quercetin pentoside, respectively³¹. Consequently, peak 46 is assigned as quercetin, molecular ion at *m/z* 301, its mass spectra was in agreement with the fragmentation pattern of quercetin aglycone, [M-H-CO]⁻ (*m/z* 273) and [M-H-CO₂]⁻ (*m/z* 257)³¹.

Peak 38, displayed [M-H]⁻ *m/z* 463, was characterized as myricetin rhamnoside, supported by its MS² *m/z* 317 [M-H-146-H] due to the loss of rhamnosyl molecule, then *m/z* 179, which is in agreement with myricetin aglycone fragmentation pattern³². Another compound was detected at peak 40 assigned for (*iso*) rhamnetin, [M-H]⁻ *m/z* 316 and MS² 272 [M-H -44 amu] equivalent to CO loss and 243[M-H -44 -30] due to loss of methoxy group²⁰. Similarly, peak 47, [M-H]⁻ *m/z* 299, the main product ions were at *m/z* 284 (base peak), due to the loss of CH₃ from the methoxy group of the aglycone, and at *m/z* 255 that represents the loss of carbonyl moiety. This pattern is in consistent with diosmetin³³.

Isoflavones were represented by four peaks, showed UV absorption at λ_{max} 250-280 nm, which suggests that they might be isoflavones: peak 44,

showed a molecular ion *m/z* 253 with a an ion fragment of *m/z* 209, assigned to the loss of 44 amu (CO₂ moiety), and was identified as Diadezein³⁴. Peak 43, with molecular ion *m/z* 268 correspondings to C₁₆H₁₂O₄ and MS² fragmentation ions at *m/z* 238 [M-H-OCH₃]⁻, this is in accordance with the mass spectrum of formonetin³⁴. Peak 39, molecular ion *m/z* 431 and MS² at *m/z* 269 [M-H-162 amu] , loss of hexose moiety, and *m/z* 179 characteristic for genistein aglycone³⁵. This compound was assigned as genistein hexoside. Another peak 42 that belongs to isoflavones with 321 *m/z* and MS² *m/z* 303, 295, 279 correspondings to fragmentation of glabrene. Therefore, this compound could be characterized as glabrene³⁶. Another compound was eluted, peak 35, with [M - H]⁻ at *m/z* 449 and MS² fragments at *m/z* 303 (-146 amu loss of rhamnose), *m/z* 287 [(M-H-rhamnose-hydroxyl)], this compound was tentatively identified as astilbin (taxifolin- rhamnoside)³⁷.

Peak 30, showed molecular ion *m/z* 447 [M-H]⁻ with a characteristic fragmentation pathway for 8-C- glycoside flavonoids, MS² at *m/z* 417(-OCH₂), 357(-90 amu), so this compound was tentatively characterized as orientin (Luteolin-8-C-β-D-glucoside)³⁸.

Miscellaneous: Two peaks were identified; peak 4 and 37 with molecular ion peaks *m/z* 249 and *m/z* 423, respectively. Both were characterized tentatively from their MS² fragment ions as Oxydisuccinic acid (peak 4) and maclurin-3-C-hexoside (peak 37) and by comparing to the reported data^{39,40}.

UPLC-MS/MS analysis of PSE and GSE proved that they are rich in antioxidants such as proanthocyanidins that have a good potential as antiaging agents through their free radical scavenging activity⁴¹. Flavonoids, the largest group among plants, are reputed with their diverse activities in skin ailments; they counteract premature activation of the signaling pathway in response to UV induced damage. Polyphenols, ellagic acids as well as flavonoid and flavonol in particular quercetin which were spotted in both studied extracts (GSE & PSE) were conveyed in a previous report and evidenced to possess free radical scavenging activity, inhibition of the elastase activity, in addition to MMP expression

reduction and increase of expression of procollagen type I⁴². Moreover, condensed and hydrolyzable tannins also have antioxidant properties and thus can inhibit elastase, hyaluronidase, collagenase activity, consequently inhibit lipid peroxidation that leads to fibrillin fiber elongation to keep the elasticity of the skin intact by preventing MMP gene initiation⁴³. The aforementioned characters of tannins could reduce the environmental influence and stress to the skin. Furthermore, improvements for texture, firmness, and elasticity of the skin is achieved that leads to counteracting the dryness of the skin. Eventually, wrinkles are smoothed out; age spots vanish by time, retaining the color and skin moisture.

CONCLUSION: This study ascribes the anti-photo aging activity of the seeds of grapes and pomegranate. An insight into their phenolic-rich extracts was traced through UPLC-ESI-MS/MS, which leads to the identification of 43 metabolites. The tyrosinase inhibitory action, as well as its anti-wrinkle activity of both extracts, were attributed to their high phenolic content and the antioxidant potential of both extracts. Therefore, the seeds of pomegranate and grapes, which are considered as waste products, could be incorporated in cosmeceutical skincare products after further clinical trials.

ACKNOWLEDGEMENT: Nil

CONFLICTS OF INTEREST: The authors have no conflict to declare.

REFERENCES:

1. Rana J, Diwakar G, Evenocheck H, Schneider LM, Shenoy D, Rebhun J, Roloff S, Scholten J and Rothouse JN: Compositions including sesamin, methods of making and using the same in skin anti-aging and skin lightening applications. In: Google Patents; 2019.
2. Greer G: The change: Women, ageing and the menopause, Bloomsbury Publishing, 2018; 496.
3. Terao M and Katayama I: Local cortisol/corticosterone activation in skin physiology and pathology, *Journal of Dermatological Science* 2016; 84: 11-16.
4. Cavinato M, Waltenberger B, Baraldo G, Grade CV, Stuppner H and Jansen-Dürr PJB: Plant extracts and natural compounds used against UVB-induced photoaging 2017; 18: 499-16.
5. Pittayaprupek P, Meephansan J, Prapapan O, Komine M and Ohtsuki M: Role of matrix metalloproteinases in photoaging and photocarcinogenesis. *International Journal of Molecular Sciences* 2016; 17: 868.
6. Freitas-Rodríguez S, Folgueras AR and Lopez-Otin C: The role of matrix metalloproteinases in aging: Tissue

- remodeling and beyond. *Biochim Biophys Acta Mol Cell Res* 2017; 1864: 2015-25.
7. Fullár A, Dudás J, Oláh L, Hollósi P, Papp Z, Sobel G, Karázi K, Paku S, Baghy K and Kovalszky I: Remodeling of extracellular matrix by normal and tumor-associated fibroblasts promotes cervical cancer progression, *BMC Cancer* 2015; 15: 1-16.
 8. Krutmann J, Bouloc A, Sore G, Bernard BA and Passeron T: The skin aging exposome, *Journal of Dermatological Science* 2017; 85: 152-61.
 9. Wittenauer J, Mäckle S, Sußmann D, Schweiggert-Weisz U and Carle R: Inhibitory effects of polyphenols from grape pomace extract on collagenase and elastase activity. *Fitoterapia* 2015; 101: 179-187.
 10. Khwairakpam AD, Bordoloi D, Thakur KK, Monisha J, Arfuso F, Sethi G, Mishra S, Kumar AP and Kunnammakkara AB: Possible use of *Punica granatum* (Pomegranate) in cancer therapy. *Pharmacological Research* 2018; 133: 53-64.
 11. Ezzat SM, Salama MM, ElMeshad AN, Teaima MH and Rashad LA: HPLC-DAD-MS/MS profiling of standardized rosemary extract and enhancement of its anti-wrinkle activity by encapsulation in elastic nanovesicles. *Archives of Pharmacol Research* 2016; 39: 912-25.
 12. Zhen J, Villani TS, Guo Y, Qi Y, Chin K, Pan M-H, Ho C-T, Simon JE and Wu Q: Phytochemistry, antioxidant capacity, total phenolic content and anti-inflammatory activity of *Hibiscus sabdariffa* leaves. *Food Chemistry*, 2016; 190: 673-80.
 13. Maciel EN, Soares IN, da Silva SC and de Souza GL: A computational study on the reaction between fisetin and 2, 2-diphenyl-1-picrylhydrazyl (DPPH), *Journal of Molecular Modeling* 2019; 25: 103.
 14. Di Petrillo A, González-Paramás AM, Era B, Medda R, Pintus F, Santos-Buelga C and Fais A: Tyrosinase inhibition and antioxidant properties of *Asphodelus microcarpus* extracts, *BMC Complementary and Alternative Medicine* 2016; 16: 453.
 15. Koh EK, Kim JE, Go J, Song SH, Sung JE, Son HJ, Jung YJ, Kim BH, Jung YS and Hwang DYJI: Protective effects of the antioxidant extract collected from *Styela clava* tunic on UV radiation-induced skin aging in hairless mice. *Int J Mol Med* 2016; 38: 1565-77.
 16. Burger P, Landreau A, Azoulay S, Michel T and Fernandez XJC: Skin whitening cosmetics: Feedback and challenges in the development of natural skin lighteners. *Cosmetics* 2016; 3: 36.
 17. Ammar S, del Mar Contreras M, Belguith-Hadrih O, Segura-Carretero A and Bouaziz M: Assessment of the distribution of phenolic compounds and contribution to the antioxidant activity in Tunisian fig leaves, fruits, skins and pulps using mass spectrometry-based analysis, *Food Funct* 2015; 6: 3663-77.
 18. Stój A, Szwajgier D, Baranowska-Wójcik E and Domagala DJSJAOE: Viticulture, Gentisic acid, salicylic acid, total phenolic content and cholinesterase inhibitory activities of red wines made from various grape varieties. *South African Journal of Enology and Viticulture* 2019; 40: 1-12.
 19. da Silva Padilha CV, Miskinis GA, de Souza MEO, Pereira GE, de Oliveira D, Bordignon-Luiz MT, dos Santos Lima MJFc, Rapid determination of flavonoids and phenolic acids in grape juices and wines by RP-HPLC/DAD: Method validation and characterization of commercial products of the new Brazilian varieties of grape. *Food Chem* 2017; 228: 106-15.
 20. Abu-Reidah IM, Ali-Shtayeh MS, Jamous RM, Arráez-Román D and Segura-Carretero A: HPLC-DAD-ESI-

- MS/MS screening of bioactive components from *Rhus coriaria* L. (Sumac) fruits. Food Chem 2015; 166: 179-91.
21. Farag M, Ezzat S, Salama M and Tadros MJ: analysis b, Anti-acetylcholinesterase potential and metabolome classification of 4 *Ocimum* species as determined via UPLC/qTOF/MS and chemometric tools. J Pharm Biomed Anal 2016; 292-302.
 22. Ruan J, Yan J, Zheng D, Sun F, Wang J, Han L, Zhang Y and Wang TJM: Comprehensive chemical profiling in the ethanol extract of *Pluchea indica* aerial parts by Liquid Chromatography/Mass Spectrometry Analysis of Its Silica Gel Column Chromatography Fractions. Molecules 2019; 24: 2784.
 23. Seraglio SKT, Valesse AC, Daguer H, Bergamo G, Azevedo MS, Gonzaga LV, Fett R, Costa ACOJFRI, Development and validation of a LC-ESI-MS/MS method for the determination of phenolic compounds in honeydew honeys with the diluted-and-shoot approach Food Research International 2016; 60-67.
 24. Scorrano S, Lazzoi MR, Mergola L, Di Bello MP, Del Sole R and Vasapollo G: Anthocyanins profile by Q-TOF LC/MS in *Myrtus communis* berries from salento area, Food Analytical Methods 2017; 10: 2404-11.
 25. Wojdyło A, Samoticha J, Nowicka P and Chmielewska J: Characterisation of (poly) phenolic constituents of two interspecific red hybrids of Rondo and Regent (*Vitis vinifera*) by LC-PDA-ESI-MS QToF. Food Chemistry 2018; 239: 94-101.
 26. Yang M, Ma Y, Wang Z, Khan A, Zhou W, Zhao T, Cao J, Cheng G and Cai S: Phenolic constituents, antioxidant and cytoprotective activities of crude extract and fractions from cultivated artichoke inflorescence. Industrial Crops and Products 2020; 143: 111433.
 27. Wojdyło A, Samoticha J, Nowicka P and Chmielewska J: Characterisation of (poly) phenolic constituents of two interspecific red hybrids of Rondo and Regent (*Vitis vinifera*) by LC-PDA-ESI-MS qTOF, Food Chem 2018; 239: 94-101.
 28. Yuzuak S, Ballington J, Xie D-YJM, HPLC-qTOF-MS/MS-Based Profiling of Flavan-3-ols and Dimeric Proanthocyanidins in Berries of Two Muscadine Grape Hybrids FLH 13-11 and FLH 17-66, Metabol 2018, 8: 57.
 29. Derakhshan Z, Ferrante M, Tadi M, Ansari F, Heydari A, Hosseini MS, Conti GO and Sadrabad EK: Antioxidant activity and total phenolic content of ethanolic extract of pomegranate peels, juice and seeds. Food and Chemical Toxicology 2018; 114: 108-11.
 30. Chen XX, Shi Y, Chai WM, Feng HL, Zhuang JX and Chen QX: Condensed tannins from *Ficus virens* as tyrosinase inhibitors: structure, inhibitory activity and molecular mechanism, PLoS One 2014; 9.
 31. Kuhnert MGEKaN: UPLC-ESI-QTOF-MS/MS Characterization of Phenolics from *Crataegus monogyna* and *Crataegus laevigata* (Hawthorn) leaves, fruits and their herbal derived drops (Crataegutt Tropfen). Journal of Chemical Biology and Therapeutics 2016; 1.
 32. Chen Y, Yu H, Wu H, Pan Y, Wang K, Jin Y and Zhang CJM: Characterization and quantification by LC-MS/MS of the chemical components of the heating products of the flavonoids extract in *Pollen typhae* for transformation rule exploration. Molecules 2015; 20: 18352-66.
 33. Akimoto N, Ara T, Nakajima D, Suda K, Ikeda C, Takahashi S, Muneto R, Yamada M, Suzuki H and Shibata DJSr: Flavonoid Search: A system for comprehensive flavonoid annotation by mass spectrometry. Scientific Reports 2017; 7: 1-9.
 34. Ren Q, Wang J, Liu S, Wang F and Wang H: Identification and determination of isoflavones in germinated black soybean sprouts by UHPLC-Q-TOF-MS mass spectrometry and HPLC-DAD. International Journal of Food Properties 2017; 20: 2877-87.
 35. Kašparovská J, Dadáková K, Lochman J, Hadrová S, Křížová L and Kašparovský T: Changes in equol and major soybean isoflavone contents during processing and storage of yogurts made from control or isoflavone-enriched bovine milk determined using LC-MS (TOF) analysis. Food Chemistry 2017; 222: 67-73.
 36. Raju KSR, Kadian N, Taneja I and Wahajuddin MJPR: Phytochemical analysis of isoflavonoids using liquid chromatography coupled with tandem mass spectrometry. Phytochemistry Reviews 2015; 14: 469-98.
 37. Chen SD, Lu CJ and Zhao RZ: Qualitative and quantitative analysis of *Rhizoma Smilacis glabrae* by ultra high performance liquid chromatography coupled with LTQ OrbitrapXL hybrid mass spectrometry, Molecules 2014; 19: 10427-39.
 38. Chen G, Li X, Saleri F and Guo M: Analysis of Flavonoids in *Rhamnus davurica* and its antiproliferative activities, Molecules 2016; 21.
 39. Fromentin Y, Cottet K, Kritsanida M, Michel S, Gaboriaud-Kolar N and Lallemand MC: *Symphonia globulifera*, a widespread source of complex metabolites with potent biological activities, Planta Med 2015; 81: 95-107.
 40. Ray A, Gupta SD and Ghosh S: Evaluation of anti-oxidative activity and UV absorption potential of the extracts of *Aloe vera* L. gel from different growth periods of plants, Industrial Crops and Products 2013; 49: 712-19.
 41. Yang L, Xian D, Xiong X, Lai R, Song J, Zhong JJBri, Proanthocyanidins against oxidative stress: from molecular mechanisms to clinical applications. BioMed Research International 2018; 12: 1-11.
 42. Im DS, Lee JM, Lee J, Shin HJ, No KT, Park SH and Kim KJAbebS: Inhibition of collagenase and melanogenesis by ethanol extracts of *Orostachys japonicus* A. Berger: possible involvement of Erk and Akt signaling pathways in melanoma cells. Acta Biochim Biophys Sin (Shanghai) 2017; 49: 945-53.
 43. Garg CJIJoGP: Molecular mechanisms of skin photoaging and plant inhibitors. International Journal of Green Pharmacy 2017; 11.

How to cite this article:

Odah SM, Salama MM, Aziz WM, El-Alfy TS and Ezzat SM: Anti-wrinkle activity and UPLC-MS/MS metabolic profiling of pomegranate and grape seeds extracts. Int J Pharm Sci & Res 2020; 11(8): 3679-89. doi: 10.13040/IJPSR.0975-8232.11(8).3679-89.

All © 2013 are reserved by the International Journal of Pharmaceutical Sciences and Research. This Journal licensed under a Creative Commons Attribution-NonCommercial-ShareAlike 3.0 Unported License.

This article can be downloaded to **Android OS** based mobile. Scan QR Code using Code/Bar Scanner from your mobile. (Scanners are available on Google Playstore)